Feasibility Study: Time-of-Flight Measurements of a Proton Beam with the Timepix4 ASIC

Particle Physics Bachelor Research Project

Author:
María Plana

Examiners:
Dr. K.A.M. De Bruyn
Dr. M.C. van Veghel

Abstract

Proton therapy is one of the most promising treatments in the oncology field. However, the lack of precise energy measurements in real-time limits future developments in this form of therapy. Providing accurate real-time measurements can boost the field. This research studies the feasibility of the time-of-flight approach to measure the energy of proton beams using two-hybrid pixel detectors formed by a silicon sensor chip and a Timepix4 readout chip at the AGOR cyclotron facilities. A simulation in Python was developed to generate and manipulate the data. Then, a toy study was performed to determine the expected precision as a function of the measuring time. Ultimately, the results show that a 4 ps precision can be achieved after 1.754 μs for a 180 MeV proton beam with a flux of 10^8 protons $s^{-1}cm^{-2}$.

Acknowledgments

I would like to thank Kristof for allowing me to briefly join the LHCb group and for giving me the opportunity to work on a topic as beautiful as proton therapy. Thank you for guiding me through a world of toy studies, accelerators and silicon pixel detectors, and feeding my interest in particle physics. I cannot imagine a better way to put an end to my bachelor's studies.

I would also like to thank my family for giving me nothing but unconditional support and opportunities, for giving me comfort and for accompanying me through this journey, even in the distance. To my dad, thank you for showing me the wonders of science from a very young age and for always believing in me.

Lastly, I would like to thank all the people who have shared adventures with me during these past three years, inspired me and brought me joy during uncertain times.

Contents

1 Introduction

Everything comes down to particle physics. From the air we breathe to the stars we watch at night, life as we know it is made of particles. Understanding particles implies understanding Nature. Although we are far from fully understanding the physics behind the smallest pieces of the puzzle, the bits we understand already have many practical applications ranging from monitoring nuclear waste to diagnosing diseases and everything in between.

One of the most used treatments for cancer currently being administered in hospitals, radiation therapy, is purely particle physics. Radiation first entered the medical field with the discovery of X-rays by W. Roentgen in 1896. It began to be used as a form of therapy shortly after by targeting cancerous tumours with high-energy X-rays to attack the DNA of cancer cells [1]. To this day, photon beams are still the most common method used for radiation delivery in hospitals [2].

Radiation therapy has excellent potential as a non-invasive treatment for cancer, and the results show success rates that are generally above 90 per cent [3]. However, further research suggests that many improvements could make radiation therapy even more efficient. Due to the importance of its use, the field is highly researched and constantly receiving upgrades. Less than a century ago, in 1946, R. R. Wilson indicated the advantages of the clinical use of proton beams over the use of photon beams, and proton therapy began to be delivered to oncology patients in the following decade [1].

Over the years, the many benefits of proton therapy have been proven. This type of beam allows for a much more precise form of treatment. High-energy protons have a limited range because they lose energy due to ionisation. As charged particles, when protons travel through matter, they have to give up energy because of their interaction with the atoms due to the stopping power of the material, parameterised as $S(E) = -\frac{\mathrm{d}E}{\mathrm{d}x}$ [4]. The ionisation cross-section is inversely proportional to the particle's kinetic energy and velocity, which implies that it deposits most of its energy towards the end of its trajectory. For this reason, there is a peak in the dose right before the particle comes to rest, known as the Bragg peak, illustrated in Figure 1a.

In treatment, a combination of Bragg peaks at different energies to cover the depth of the tumour, known as a spread-out Bragg peak (SOBP) [1], is set to coincide with the position of the cancerous cells, as shown in Figure 1b. Since the ionisation loss is still minor as the proton traverses healthy tissue, it receives minimal radiation. This fact makes proton beams a much more localised treatment and aggressive on the tumour while protecting the healthy tissue around it to a great extent. As illustrated in Figure 1b, the dose profile of the proton beam differs significantly from that of the photon beam, where the maximum dose is delivered just below the surface, not at the tumour location necessarily.

The clinical use of proton therapy is already showing promising results with minor collateral damage in patients, but scientists keep working to improve the technology that delivers it.

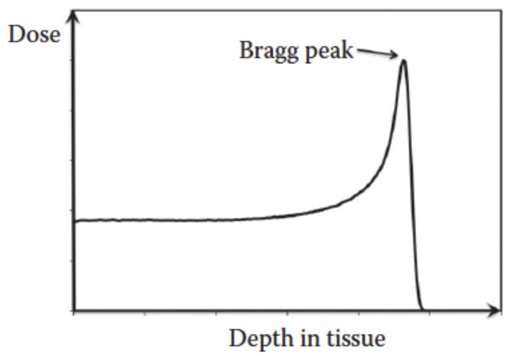

(a) Bragg peak. Image taken from Ref.[1]

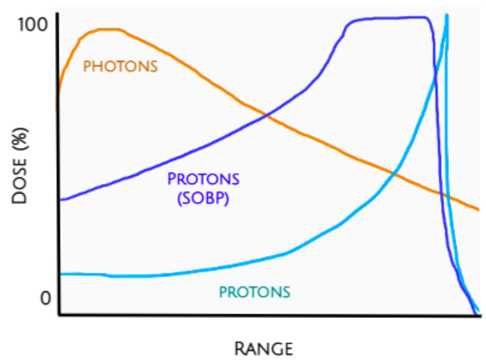

(b) Dose distribution in radiation therapies.

Figure 1: Delivered radiation doses.

From the physics side, it is clear that the Bragg peak's position depends on the proton's initial velocity and kinetic energy when it begins to penetrate the ionising material, in this case, the tissue. The limiting factor when it comes to taking these measurements is the precision with which we know the energy of the protons in the beam. The beam energy is usually calibrated by measuring the penetration depth of the protons in water, their range [5]. However, such a calibration method lacks precision and can hardly be improved, especially for protons with smaller ranges.

To keep improving the precision of the treatment and to adjust the radiation doses further, the real-time energy and velocity of the protons would have to be identified by following a different path. A way to achieve these measurements is to record the time it takes for individual protons to travel a known distance between two detectors, their time of flight, instead of their range. As opposed to traditional calibrating techniques, such a method would improve overall precision, even for less-energetic protons.

The required clinical precision for these time-of-flight measurements has to range between 90 ps for a 60 MeV proton beam and 4 ps for a 230 MeV beam, both for a 1 m distance between the detectors [6]. Such precision can not yet be achieved with the current commercialised technology. However, the new fast timing detectors under development for the next generation of high-energy physics experiments are expected to achieve this precision.

One of the prime candidates for time-of-flight measurements in real-time is the Timepix4 readout ASIC, which will be the newest addition to the ASIC family developed by the Medipix Collaboration, hosted by CERN in Geneva and Nikhef in Amsterdam. The readout chip is combined with a silicon sensor chip to make a silicon pixel hybrid detector. The resolution achieved by the new models has already been significantly improved, and it is expected to be in the order of 100 ps [7]. The present research project explores whether the 100 ps precision expected from a Timepix4-based silicon detector is enough for time-of-flight measurements in real-time, as described above. The use of simulations coded in Python has determined the feasibility of these measurements. Additionally, the investigation has been oriented toward designing a future experiment at Groningen's AGOR cyclotron accelerator facilities.

2 Research Strategy

2.1 Theoretical Time of Flight

In therapy, proton beams have kinetic energies that range from 60 MeV to 230 MeV [6]. This research aims to explore the feasibility of future experiments that might take place at the AGOR cyclotron accelerator, which can only produce stable particle beams with energies up to 184 MeV, as mentioned on their website [8]. Therefore, the target of the developed simulations has been a beam with kinetic energy equal to 180 MeV.

Protons with kinetic energies as high as 180 MeV are given the relativistic treatment because Newtonian equations are not good enough to describe the system. There are two relevant equations from special relativity for this, Equation 1 and Equation 2. The first one is the reduced kinetic energy, τ, and is given by the quotient between the kinetic energy, E, and the rest mass energy, mc^2, where m is the rest mass of the proton and c is the speed of light. The second one, β, is the ratio of the particle's velocity to the speed of light and is given by τ. Therefore, $\tau = 0.192$ and $\beta = 0.544$ for the given case where E = 180 MeV means that such protons travel with a velocity slightly above half the speed of light.

$$\tau = \frac{E}{m_p c^2} \tag{1}$$

$$\beta^2 = \frac{\tau + 2}{(\tau + 1)^2}\tau \tag{2}$$

The time-of-flight of the individual protons can be calculated from the distance they travel, d, and the velocity at which they do it, v. The former was assumed to be 1 m throughout this research, while the latter can be obtained from Equation 3 and has a value of approximately $v = 1.6 \cdot 10^8$ ms^{-1} for this specific case. The time-of-flight, ToF, is simply the ratio of distance travelled to velocity, as shown in Equation 4.

$$v = c\beta \tag{3}$$

$$ToF = \frac{d}{v} \tag{4}$$

So far, all the relationships given in this section can be combined to obtain an expression of time-of-flight as a function of the proton's initial kinetic energy, E, and the distance travelled, d. This equation provides a more straight-forward approach and is shown in Equation 5 [6].

$$ToF(E, d) = \frac{(E + mc^2)d}{c\sqrt{(E + mc^2)^2 - m^2c^4}} \tag{5}$$

Finally, it can be concluded that a proton with 180 MeV kinetic energy travels 1 m in 6.130861 ns, ignoring energy losses that arise from traversing the detector planes and the air between them. Although energy losses of protons are well known for air and silicon, they have been ignored in this research.

2.2 Required Clinical Precision

Real-time time-of-flight measurements will significantly impact how the particle beams used to deliver proton therapy are calibrated. Additionally, they will offer real-time tracking of the radiation doses administered to patients. Supposing this tracking technique could be matched in the future with a fast response in the control of the beam, the doses could be adjusted fast enough to limit the amount of radiation administered during treatment to a considerable extent.

The maximum clinical tolerance on the range uncertainty, the range of the proton once it has penetrated the tissue, is usually less than 1 mm, which translates to a 4 ps uncertainty in the time-of-flight of a 230 MeV proton beam being tracked for 1 m [6]. This research aims to show that the expected uncertainty of the 180 MeV proton beam can be kept below this threshold of 4 ps using the Timepix4.

2.3 The Detector

The proposed setup includes a beam accelerated in the AGOR cyclotron, which then leaves the accelerator and passes through two detectors placed 1 m apart from each other that will measure the time-of-flight of the individual protons, as mentioned earlier.

The devices employed to take the measurements are hybrid pixel detectors, illustrated in Figure 2. These have two main layers. The first layer is a semiconductor sensor chip made out of silicon. It serves to detect the particle by collecting the ionisation charge left by the passing charged particles and creating an electrical signal. The second layer consists of a readout chip, the Timepix4 ASIC. It converts the electrical signal to a digital one, recording the location and time of the hit.

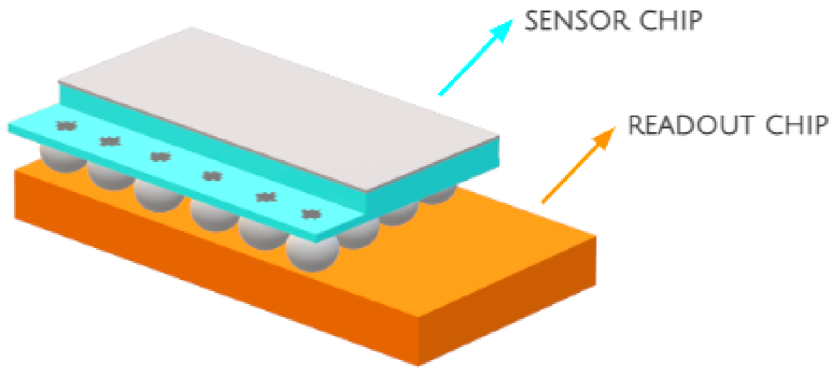

Figure 2: Hybrid pixel detector with a silicon sensor chip and a Timepix4 readout chip.

The Timepix4 consists of pixels with sizes of 55 × 55 μm^2 that form a 448 × 512-pixel matrix, as in the most recent published papers [9]. The silicon chip size is precisely the same, so the hybrid detector has an active detection area of 7.41 cm^2.

The design of the Timepix4 has been significantly improved and offers a much better timing resolution than previous generations of readout chips. However, one of its most significant assets is the chip's time resolution. The model's time-to-digital converter, TDC, can reach a precision of around 60 ps [7]. Adding to this the timing effects of the complete sensor, the lower limit of the best achievable front-end time resolution is 88 ps [7] for the hybrid pixel detector. This report assumed an estimate of 100 ps time resolution to prove that it is enough to take real-time time-of-flight measurements.

3 Simulating a Time-of-Flight Measurement

This research carried out a series of simulations to understand the ability to take time-of-flight measurements with a 4 ps precision of the Timepix4 hybrid detector, with a 100 ps resolution. For this proof-of-concept, all the data corresponding to the proton beams has been generated and does not correspond to actual measurements.

3.1 Description of a Single Measurement

The theoretical time-of-flight of a single proton is not a good representation of the measurements the detectors would take. Theoretically, all protons within a beam should produce the exact time-of-flight measurements, but this is not the case in practice. Many factors can cause a spread in the individual measurements. For instance, not all the protons within the beam have the same energy, but this research does not explore the case. However, the leading cause for the spread is the detectors' time resolution, which is this report's primary focus.

Due to the resolution of the detectors, the measurements of a single-energy proton beam will not result in a single value. Instead, they will give a spread of values around the theoretical time of flight. The best approach to these results is a normal distribution with a mean, μ, equal to the theoretical time value and a standard deviation, σ, corresponding to the time resolution of the detector, namely 100 ps in this study.

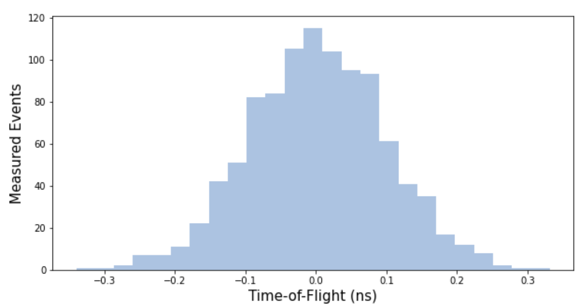

(a) Detector 1

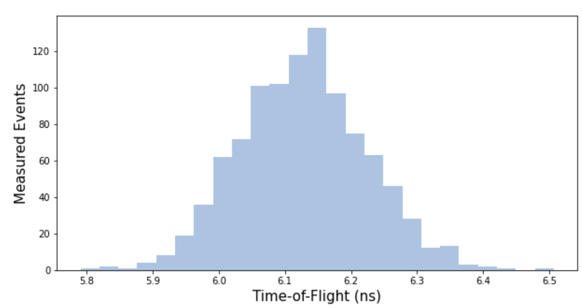

(b) Detector 2

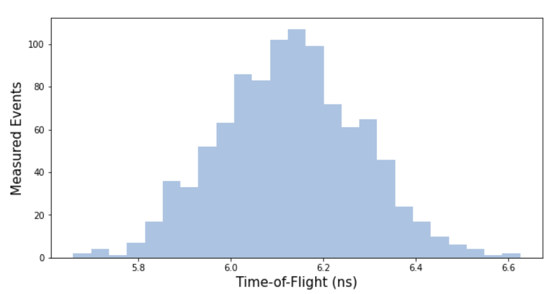

(c) Time-of-flight

Figure 3: Time measurements after 1000 events as recorded by detectors in the simulated setup.

In the chosen reference frame, t = 0 is when a single proton with 180 MeV kinetic energy hits the first detector. The proton hits the second detector after the calculated time-of-flight, 6.13 ns. These measurements are recorded as random time points within the normal distributions with $\mu = 0$ ns and $\sigma = 0.1$ ns in the case of the first detector, and $\mu = 6.13$ ns and $\sigma = 0.1$ ns in the case of the second detector. The times are then combined to give the total time of flight. If this procedure is carried out multiple times, the data of a proton beam is generated.

This research works with the number of events measured, which refers to the number of protons hitting both detectors. For instance, Figure 3a shows the distribution of the time measurements after the first detector has measured 1000 events, while Figure 3b shows the same for the second detector. The time difference between these two gives the time-of-flight measurements, shown in Figure 3c.

3.2 Fitting the Data

A more significant number of measurements leads to results closer to the actual value and less spread out. This fact is illustrated in Figure 3, as the individual hits do not reach the desired precision, but the combined information of all the events peaks at the true value, giving a more accurate estimate. However, measurements take time, which results in more extended waiting periods to obtain the desired precision. This research aims to determine the balance between the measuring time and the expected precision, which starts by finding out the number of events needed to achieve a time precision of 4 ps.

The data produced by the detectors, as shown in Figure 3, can then be fitted to a Gaussian distribution, Equation 6, to obtain the parameters μ and σ from the fit, as well as their respective uncertainties. These parameters are interpreted as the measured time-of-flight after a specific number of measurements and the spread around this value, respectively. The larger the number of measurements taken, the smaller the uncertainty on the mean of the fit will be and the better the estimate of the time-of-flight measurement.

$$f(x) = \frac{1}{\sigma\sqrt{2\pi}} e^{\frac{1}{2}(\frac{x-\mu}{\sigma})^2} \tag{6}$$

In order to find these optimised parameters, a fit using the unbinned maximum likelihood estimation method of the histogram has been carried out. This fit has been done by applying the MIGRAD minimisation algorithm from the numerical minimisation library MINUIT. The relevant retrieved results given by the fitting tool are the parameters μ and σ with their respective errors, σ_μ and σ_σ, obtained from the covariance matrix. The parameters μ and σ are calculated from the array to provide an initial guess to stop the algorithm from taking an invalid function minimum.

An example of the final result of the fit is shown in Figure 4a for 1000 events and Figure 4b for 2000 events. In the former case the optimized mean parameter is $\mu = 6.1286 \pm 0.0045$ ns, while in the latter $\mu = 6.1347 \pm 0.0032$ ns. This proves that more events lead to better precision, which is a consistent pattern for any number of measurements.

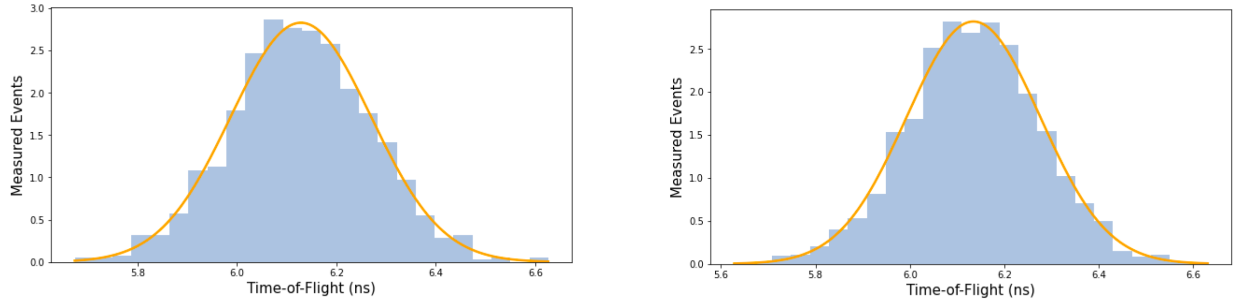

(a) 1000 recorded events

(b) 2000 recorded events

Figure 4: Normal fit functions according to optimized parameters μ and σ.

The method described in this section to obtain the time-of-flight measurements has been used to generate data samples for different numbers of events ranging from 1000 to 2000. The means and their errors obtained from the fits can then be compared for the different cases to determine the number of measurements needed to obtain results with the desired precision.

3.3 Toy Study

For single measurements, whether actual or simulated, the sample and the time-of-flight values obtained from the mean of the fit fluctuate. Consequently, the individual recorded values are not representative of the expected response of the measurement setup. A toy study can be performed to get a better picture of the expected response despite the fluctuations in the individual measurements. In such a study, the samples are drawn repeatedly to analyse the overall output that number of events gives.

In this case, the toy study has been performed for a number of events ranging from 1000 to 2000. The data samples have been generated 1000 times for each case, meaning 1000 toys, and once again plotted as histograms. The fit method explained earlier has been carried out to obtain the mean and the standard deviation, as well as their errors, for every single one of all the generated toys. All the obtained mean values, μ, and their uncertainties, σ_μ, have been combined. Then, another fit has been performed to obtain the mean of the means μ_μ, and its error, σ_{μ_μ}, from all the toys. This last value, the mean of the means, should correspond to the theoretical time-of-flight, 6.13 ns. This value provides a cross-check of the analysis to search for potential fit biases.

Figure 5 shows an example of this fitting, where a toy study has been performed for 1000 events and 1000 toys. For this specific case, the time-of-flight value obtained from the fit is $\mu_\mu = 6.1311 \pm 0.0001$ ns. This mean is now statistically significant and is considered the achieved time-of-flight value after 1000 measurements. The obtained values for σ and σ_σ are not relevant for this method. This procedure has then been applied to obtain the rest of the estimated values for the different number of events. The calculated time-of-flight values for a number of events ranging from 1000 to 2000 can be found in Appendix A.1.

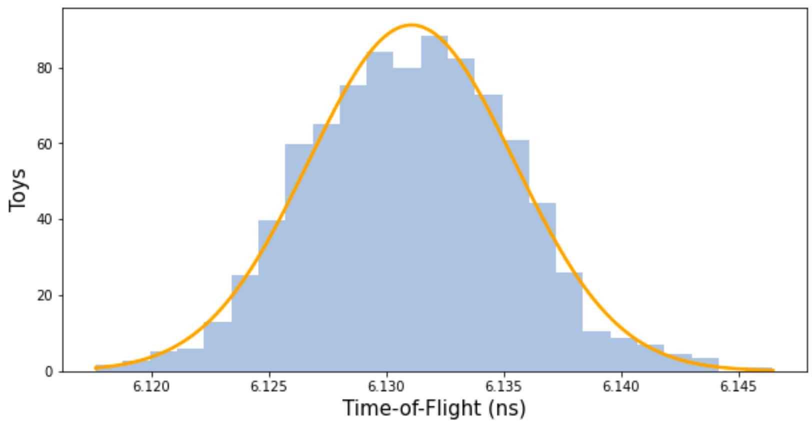

Figure 5: Fitted toy model for 1000 events and 1000 toys.

Similarly, the errors on the means, σ_μ, obtained from the toy study, are plotted and fitted. The mean of the error on the means, μ_{σ_μ} is the expected precision obtained after a number of measurements, thus the critical parameter of interest in this research. This topic is explained more thoroughly in Section 3.4.

3.3.1 Pull

The reliability of the toy study can be put to the test by calculating the pull. The pull aims to portray the validity of the toy study by showing the deviation of the measured value from the true value. Also, it shows whether the error has been underestimated or overestimated, and it can be calculated following Equation 7, considering the means and their errors from each toy.

$$pull = \frac{\mu - ToF}{\sigma_\mu} \tag{7}$$

Then, the pull is plotted as a histogram and fitted using the same method described above, as shown in Figure 6. Ideally, the optimised fit parameters for a perfect toy model would be that of the standardised normal distribution with $\mu = 0$ and $\sigma = 1$. The results after fitting the pull from the performed toy study in this research are $\mu = 0.0107 \pm 0.001$ and $\sigma = 1.0055 \pm 0.007$, meaning that the results of the study are slightly biased but are valid as these are what could be expected from a fair estimate.

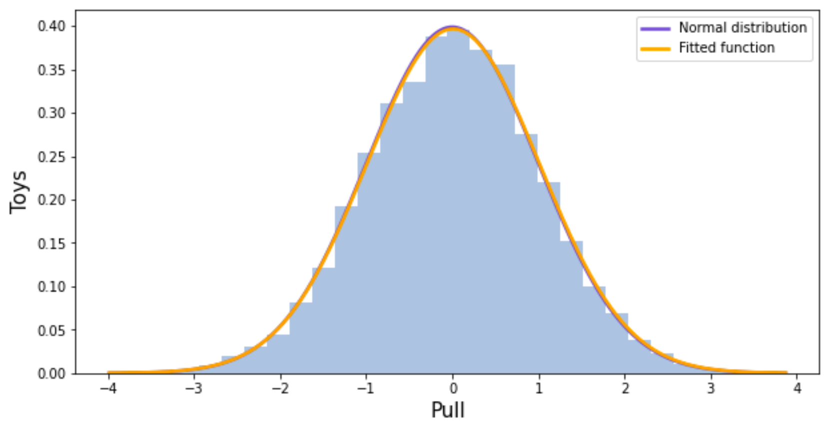

Figure 6: Fit of the pull and plot of standardized normal distribution for comparison.

3.4 Sensitivity Study

As mentioned earlier, the aim is to reach a precision below 4 ps using the Timepix4 for time-of-flight measurements. The greater the number of measured events, the more precise the measurement. The toy study provides a better estimate of the expected precision after a number of events. The sensitivity study analyses the error of the mean from each data sample.

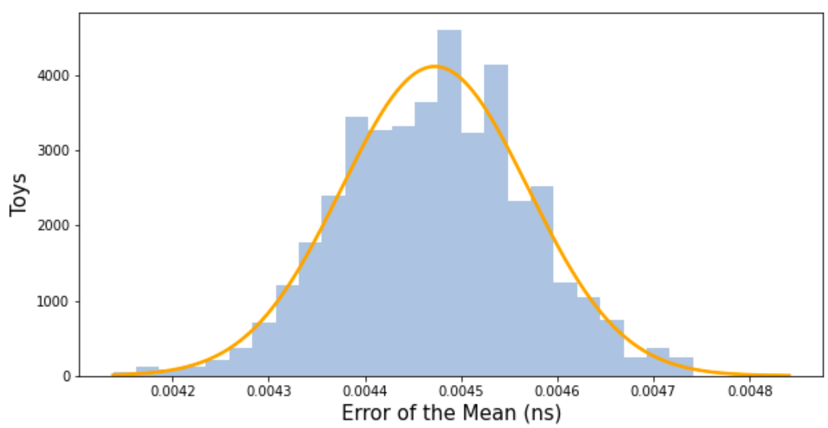

Figure 7: Fit of σ_μ after 1000 events and 1000 toys.

This time, the histograms are plotted for the σ_μ values, as shown in Figure 7 for 1000 events. Then, μ_{σ_μ} and σ_{σ_μ} are obtained from the fit. The former gives an estimate of the expected precision obtained after a number of measurements, while the latter is simply the spread of that precision. These two can be plotted against the number of measurements to get an overview of the precision the measurements can achieve. The final results are shown in Figure 8. All of the values obtained from the fits used to make this plot can be found in Appendix A.2.

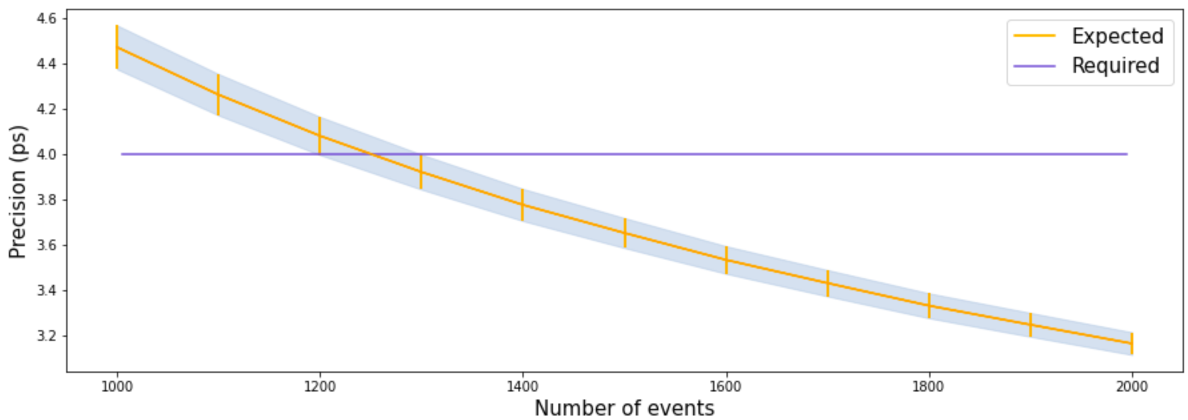

Figure 8: Expected precision as a function of the number of events recorded after toy study.

This last plot is a good representation of the expected precision per number of measurements. The straight line represents the desired precision of 4 ps, achieved after 1250 measurements. However, the error bar is still slightly above the desired value, meaning that 1300 measurements would be the safest choice to determine the time-of-flight of the protons with the desired precision.

3.4.1 Required Measuring Time at AGOR

The AGOR facility is the result of a collaboration between PARTREC in the Netherlands and IPN in France. The accelerator consists of a superconducting cyclotron capable of accelerating protons and selected heavy ions. The PARTREC facility is managed by the UMCG in Groningen and produces beams with a theoretical maximum of 190 MeV. However, this value is reduced to 184 MeV for stable beams. Additionally, such beams are generated with fluxes ranging from 10^4 to 10^8 protons $s^{-1}cm^{-2}$ [8], but proton therapy uses beams that range from 10^8 to 10^{10} protons $s^{-1}cm^{-2}$. Therefore, this research focuses in a proton beam of 10^8 protons $s^{-1}cm^{-2}$.

Keeping in mind that the sensitive area of the detector is equal to 7.41 cm^2, and assuming a detection efficiency equal to 1, the detectors would record $7.41 \cdot 10^8$ protons s^{-1} if the produced flux were to be of 10^8 protons $s^{-1}cm^{-2}$. The horizontal axis from the plot in Figure 8 can be translated into seconds using the protons-per-second relationship. This relationship leads to a plot like the one shown in Figure 9, where the expected precision can be studied in terms of the time it would take to achieve such precision.

This last plot concludes the research by showing that the desired precision can be obtained after 1.619 μs, keeping in mind the error bars of the estimate. However, the measurement, including its error, is not below the limit of the required precision until after 1.754 μs.

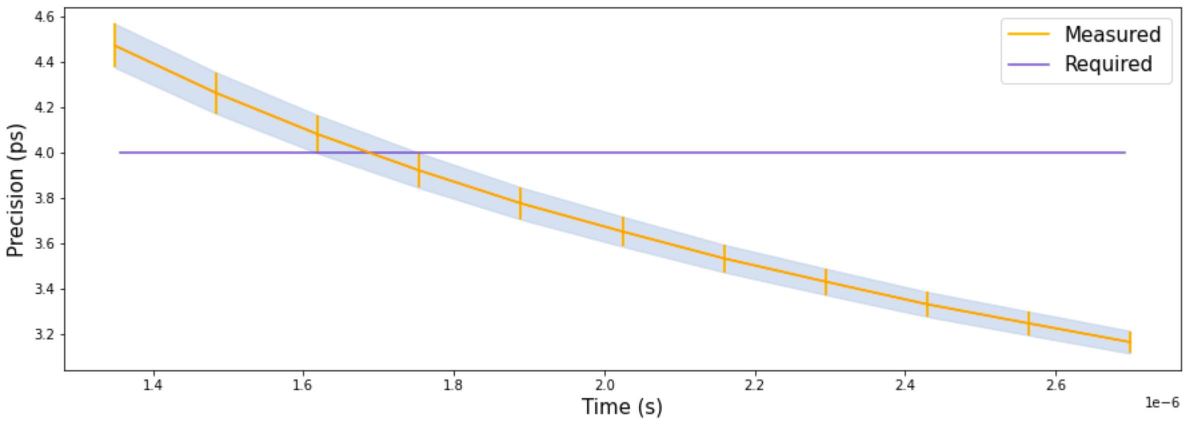

Figure 9: Expected precision as a function of the time it would take to achieve it. Assuming a flux of 10^8 protons $s^{-1}cm^{-2}$ and a sensor surface of 7.41 cm^2, matching the AGOR accelerator and the Timepix4 sensor.

4 Outlook

This research aims to determine whether the time precision of the Timepix4 ASIC, which is estimated to be in the order of 100 ps, is enough to take real-time time-of-flight measurements of proton beams. A toy study has been performed to obtain the results used to find the expected time precision per number of measurements. It has been shown that after the detectors record 1300 events, the expected precision is below the 4 ps threshold. Additionally, this number has been translated into measuring time at AGOR for a proton beam of 10^8 protons $s^{-1}cm^{-2}$. From this plot, it can be concluded that after 1.754 μs of measuring time, the expected precision of the time-of-flight measured value is kept below 4 ps.

In order to interpret the results and understand whether the research outcome is positive, the concept of "real-time" still has to be defined. In a practical and ordinary situation, real-time can never be immediate. Even the fastest known traveller, light, takes time to wander over some distance. The same happens in the case of proton therapy; the detectors take some time to generate a signal, and machines take some time to react to this signal. Instead of attempting to take these measurements in no time, a more realistic approach is to determine a time limit that is good enough to be considered real-time. In this case, a good starting point is to look at the time the machines take to react and rectify the energy of the beam they are producing. In the case of the experiments carried out by PARTREC regarding proton therapy, this time is greater than 1 s. For this research and until this reaction time can be improved, anything below the 1 s limit is considered real-time.

Returning to the results of this research, the required precision is obtained only after 1.754 μs. This value, which is well below the 1 s benchmark, implies that real-time time-of-flight measurements of proton beams with a precision of at least 4 ps would be possible, given the parameters used for this research.

4.1 Assumptions and Prospective Research

This research is not exhaustive, and certain interesting aspects still need to be looked at to reach a significant conclusion on the capabilities of these hybrid detectors to measure with the specified precision.

In the first instance, it is crucial to keep in mind that the entirety of this research has been based on an optimistic guess of the detectors' time resolution. The value of 100 ps comes from various sources cited in the References section. It is based on the performance of the Timepix4 at the moment, which has the best achievable front-end time resolution of 88 ps [7]. This value estimate is not binding and would need to be revisited once the Timepix4 has been finalised and commercialised. However, the code developed for this research allows for easy modification and could be adapted once the exact resolution has been determined.

The whole research relies on the ability of the detectors to recognise coincident signals. This means that some mechanism tells the protons apart and identifies and matches the individual signals that the protons produce on each detector. This subject could be a research project topic and is currently out of this research's range, but it is important to note that the investigation could not have been done if this were not the case. Furthermore, it is assumed that there is no scattering from the beam, meaning that the protons travel parallel to each other within the beam following a straight line and that the detectors are correctly aligned.

Additionally, the research assumes that the detectors never reach a saturation point and have a detection efficiency of 1. All the protons that go through the detection planes are correctly recognised and recorded. In reality, once again, this is not often the case. Additionally, the efficiency depends mainly on the density of the hits and the dead time of the detectors, associated with the signal reading time. A defocused beam spread over the detection area of the Timepix4 would be preferred to maximise the efficiency of the detectors. However, the beams should be as focused as possible for proton therapy. Of course, this issue is a matter for future research. However, the efficiency could be considered in the future by modifying the magnitude of the flux the detectors can recognise. This approach can also be easily changed in the written code.

Regarding the studied beam, it has been assumed that all of the protons within it carry the same kinetic energy. In reality, this is usually not the case. A proton beam generated in a facility such as the AGOR cyclotron is expected to have some spread around the requested value. For this reason, not all protons in a 180 MeV proton beam carry that same kinetic energy. This spread could also affect the time-of-flight of such protons that could have repercussions on the measurements, leading to a change in the estimated precision. However, it is expected that the results would not be entirely compromised since most protons would still carry the same energy, and the average would be kept the same. The magnitude of this spread depends on the accelerator being used, and the specifics of it could be included in future research.

To conclude this section, the research has not dealt with energy losses of any kind along the protons' trajectories. Protons lose energy due to ionisation as they traverse any medium, not only when they enter the tissue. Even though it happens to a smaller extent, energy loss occurs as they travel through the air or the detectors. The velocity of the protons is then reduced, leading to consequences in their flight time. Although important, the impact of such energy losses is expected to be minimum. This is in line with the fact that energy loss is inversely proportional to the particle's velocity; before entering the tissue, the velocity of the protons is highest. Still, energy losses are known for air and silicon. Future research and simulations should consider these factors by noting the detectors' depth to make the results more realistic and precise.

5 Conclusion

Proton therapy has proven to be one of the most effective treatments for oncology patients, showing very high success rates and very little collateral damage. However, much room for improvement requires scientists to be on the front line of research to push the limits of what is possible in radiation therapy. One of the biggest challenges in the field of proton beams is the lack of effective and precise methods to measure the energy and velocity of the high-energy protons in real-time.

The time-of-flight approach explored in this research allows for taking measurements with an expected precision below 4 ps. The Timepix4 readout chip is combined with a silicon sensor chip to compose a hybrid detector with a timing precision estimated to be around 100 ps. With such precision, the time-of-flight measurements can be obtained after 1300 measured protons or 1.754 μs at AGOR, which has been concluded to be real-time.

Although the findings of this research look very promising, there are still a lot of relevant factors that need to be accounted for to get a more realistic picture. This research has been mainly limited by the fact that there is little information about the Timepix4 as it is still undergoing the trial period. However, the simulation developed for this paper leaves enough room to make changes straightforwardly as more information becomes available in the future.

Taking real-time time-of-flight measurements would be a big step forward in the development of proton beam radiation therapy. This improvement would lead to a much more efficient method to calibrate the beam's energy and the possibility of real-time tracking of the radiation doses. Perhaps more applications, such as the adjustment of the energy of the beam during treatment, will come to light as research sprouts and we experience great leaps in technology development.

A Results of the Toy Study

A.1 Time-of-Flight

Events	μ (ns)	σ_μ (ns)	σ (ns)	σ_σ (fs)
1000	6.131073	0.000138	0.004377	97.9579
1100	6.131113	0.000141	0.004444	99.4692
1200	6.130836	0.000133	0.004206	94.1519
1300	6.130938	0.000123	0.003876	86.7725
1400	6.130621	0.000119	0.003765	84.2894
1500	6.130935	0.000112	0.003548	79.4460
1600	6.130923	0.000109	0.003434	76.9181
1700	6.131036	0.000109	0.003451	77.3000
1800	6.130705	0.000106	0.003357	75.2006
1900	6.130807	0.000107	0.003373	75.5613
2000	6.130978	0.000101	0.003185	71.3504

A.2 Expected Precision

Events	μ_{σ_μ} (ns)	$\sigma_{\mu_{\sigma_\mu}}$ (fs)	σ_{σ_μ} (fs)	$\sigma_{\sigma_{\sigma_\mu}}$ (fs)
1000	0.004473	3.06698	96.9861	2.16867
1100	0.004263	2.89268	91.4743	2.04548
1200	0.004081	2.66617	84.3115	1.88526
1300	0.003921	2.44547	77.3325	1.72921
1400	0.003775	2.24615	71.0294	1.58827
1500	0.003651	2.09625	66.2889	1.48227
1600	0.003532	1.92778	60.9614	1.36314
1700	0.003429	1.83966	58.1751	1.30084
1800	0.003329	1.74136	55.0664	1.23132
1900	0.003245	1.66613	52.6876	1.17813
2000	0.003162	1.57885	49.9274	1.11641

References

[1] Harald Paganetti. *Proton therapy physics*. CRC Press/Taylor Francis, 1 edition, 2012.

[2] Johannes A. Langendijk, Liesbeth J. Boersma, Coen R.N. Rasch, Marco van Vulpen, Johannes B. Reitsma, Arjen van der Schaaf, and Ewoud Schuit. Clinical trial strategies to compare protons with photons. *Seminars in Radiation Oncology*, 28(2):79–87, 2018.

[3] Daniel J. Indelicato, Ronny L. Rotondo, Haruka Uezono, Eric S. Sandler, Philipp R. Aldana, Nathan J. Ranalli, Alexandra D. Beier, Christopher G. Morris, and Julie A. Bradley. Outcomes following proton therapy for pediatric low-grade glioma. *International Journal of Radiation Oncology Biology Physics*, 104(1), 2019.

[4] Brian Martin. *Nuclear and Particle Physics: An Introduction*. John Wiley & Sons Ltd, 2 edition, 2009.

[5] M. F. Moyers, G. B. Coutrakon, A. Ghebremedhin, K. Shahnazi, P. Koss, and E. Sanders. Calibration of a proton beam energy monitor. *Medical Physics*, 34, 2007.

[6] A. Vignati, S. Giordanengo, F. Mas Milian, Z. Ahmadi Ganjeh, M. Donetti, F. Fausti, M. Ferrero, O. Hammad Ali, O. A.Mart Villarreal, G. Mazza, Z. Shakarami, V. Sola, A. Staiano, R. Cirio, R. Sacchi, and V. Monaco. A new detector for the beam energy measurement in proton therapy: a feasibility study. *Physics in Medicine and Biology*, 65, 2020.

[7] K. Heijhoff, K. Akiba, R. Ballabriga, M. van Beuzekom, M. Campbell, A. P. Colijn, M. Fransen, R. Geertsema, V. Gromov, and X. Llopart Cudie. Timing performance of the timepix4 front-end. 2022.

[8] Particle Therapy Research Center (PARTREC), 2022.

[9] X. Llopart, J. Alozy, R. Ballabriga, M. Campbell, R. Casanova, V. Gromov, E. H.M. Heijne, T. Poikela, E. Santin, V. Sriskaran, L. Tlustos, and A. Vitkovskiy. Timepix4, a large area pixel detector readout chip which can be tiled on 4 sides providing sub-200 ps timestamp binning. *Journal of Instrumentation*, 17, 2022.